MIT Libraries | DSpace@MIT

MIT Open Access Articles

Global precipitation retrieval algorithm trained for SSMIS using a numerical weather prediction model: Design and evaluation

The MIT Faculty has made this article openly available. ***Please share*** how this access benefits you. Your story matters.

Citation: Surussavadee, Chinnawat, and David H. Staelin. "Global Precipitation Retrieval Algorithm Trained for SSMIS Using a Numerical Weather Prediction Model: Design and Evaluation." IEEE, 2010. 2341–2344. © Copyright 2010 IEEE

As Published: http://dx.doi.org/10.1109/IGARSS.2010.5649699

Publisher: Institute of Electrical and Electronics Engineers (IEEE)

Persistent URL: http://hdl.handle.net/1721.1/72665

Version: Final published version: final published article, as it appeared in a journal, conference proceedings, or other formally published context

Terms of Use: Article is made available in accordance with the publisher's policy and may be subject to US copyright law. Please refer to the publisher's site for terms of use.

Massachusetts Institute of Technology

GLOBAL PRECIPITATION RETRIEVAL ALGORITHM TRAINED FOR SSMIS USING A NUMERICAL WEATHER PREDICTION MODEL: DESIGN AND EVALUATION

Chinnawat Surussavadee[1,2], Member, IEEE, and David H. Staelin[1], Life Fellow, IEEE

[1]Research Laboratory of Electronics, Massachusetts Institute of Technology, Cambridge, MA 02139 USA

[2]Andaman Environment and Natural Disaster Research Center, Faculty of Technology and Environment, Prince of Songkla University, Phuket Campus, Phuket 83120 Thailand

ABSTRACT

This paper presents and evaluates a global precipitation retrieval algorithm for the Special Sensor Microwave Imager/Sounder (SSMIS). It is based on those developed earlier for the Advanced Microwave Sounding Unit (AMSU) [1]-[6] and employs neural networks trained with 122 global storms that spanned a year and were simulated using the fifth-generation National Center for Atmospheric Research/Penn State Mesoscale Model (MM5) and a radiative transfer program validated using AMSU observations. Only non-icy surfaces at latitudes less than 50º have been analyzed because their surface effects are more predictable. Sensitivity to surface emissivity variations was reduced by using only more surface-insensitive principal components of brightness temperature. Based on MM5 simulations, retrievals for land are slightly less accurate than those for sea and all are useful for rates above 1 mm/h. F-16 SSMIS, NOAA-15 AMSU, and Global Precipitation Climatology Project (GPCP) annual estimates generally agree. SSMIS retrieves less precipitation for some areas partly due to its higher resolution that resolves precipitation better. SSMIS overestimates precipitation over under-vegetated land requiring the near-surface evaporation correction illustrated earlier for AMSU [6].

Index Terms— Special Sensor Microwave Imager/Sounder (SSMIS), microwave precipitation estimation, precipitation, rain, remote sensing, satellite.

1. INTRODUCTION

SSMIS [7]-[8] was first launched in October 2003 aboard the Air Force Defense Meteorological Satellite Program (DMSP) F-16 Spacecraft. Its 24-channels conically scan the Earth's surface at a constant incidence angle of 53.1° with spatial resolutions that range from 46.5 x 73.6 km at 19 GHz to 13.2 x 15.5 km at 183 GHz over the full width of its ~1700-km swath. SSMIS combines in one conically scanned dual-polarization instrument the approximate functionality of the conically scanned dual-polarization DMSP satellite Special Sensor Microwave Imager (SSMI) for surface and precipitation sounding, and the two cross-track scanned Special Sensor Microwave Sounders, SSMT-1 for temperature profiles and SSMT-2 for humidity profiles. SSMIS provides better spatial resolution than SSMT but with reduced swath width. Although the frequencies employed by SSMIS are similar to those of AMSU, problematic differences include: 1) vertical polarization was used for the SSMIS 50-GHz temperature-profile sounding channels, 2) to improve spatial resolution most SSMIS channels are diffraction limited rather than having roughly constant beamwidth across various bands, and 3) SSMIS views at a high constant zenith angle. These differences relative to AMSU contributed to revisions of the existing AMSU precipitation retrieval algorithm architecture [6] in order for SSMIS to produce successful retrievals. These algorithmic differences involve the channel-bias corrections, the channels and principal components (PCs) used, and the use of less mature SSMIS algorithms (which time will remedy).

2. SIGNAL SELECTION AND CONDITIONING

Table I shows SSMIS (S) channel specifications [7] and AMSU (A) channels with similar frequencies. Only SSMIS channels with corresponding AMSU channels were used in precipitation retrieval. SSMIS channels 6, 7, and 19-24 generally sense altitudes above precipitation and were not used. Since SSMIS channels 12 and 13 are strongly affected by surface signatures, they were also omitted. To reduce surface signals, vertically polarized channels (V-pol) were used for window frequencies that measure dual polarization. Preprocessing steps using the satellite observations included: 1) correction for biases between SSMIS and MM5 brightness temperatures (TBs), 2) determination of surface classification, and 3) computation of principal components (PCs) for surface-sensitive channels and selection of those with useful signal-to-noise (SNR) ratios. Although AMSU-based precipitation retrievals usefully exploit 53-GHz H-polarized brightness temperature perturbations due to precipitation, F-16 SSMIS V-polarized 53-GHz perturbations are smaller and were not used (F17 is H-polarized near 53 GHz). Since it views a single zenith angle, SSMIS-observed TBs were not corrected to those at nadir. Such a correction was performed for AMSU.

TABLE I
SSMIS CHANNEL SPECIFICATIONS [7] AND AMSU CHANNELS WITH SIMILAR FREQUENCIES (CHANNELS 19-24 OMITTED HERE)

S Ch.	SSMIS Freq. (GHz)	Spatial Res.	Spec. NEΔT (K)	A ch.	A Freq. (GHz)
1	50.3 (V)	37.7 × 38.8	0.4	A3	50.3 (V)
2*	52.8 (V)	37.7 × 38.8	0.4	A4	52.8 (V)
3*	53.596 (V)	37.7 × 38.8	0.4	A5	53.596 (H)
4*	54.4 (V)	37.7 × 38.8	0.4	A6	54.4 (H)
5*	55.5 (V)	37.7 × 38.8	0.4	A8	55.5 (H)
6	57.29 (R)	37.7 × 38.8	0.5	-	-
7	59.4 (R)	37.7 × 38.8	0.6	-	-
8*	150 (H)	13.2 × 15.5	0.875	B2	150 (H)
9*	183.3±6.6 (H)	13.2 × 15.5	1.2	B5	183.3±7 (V)
10*	183.31±3 (H)	13.2 × 15.5	1.0	B4	183.3±3 (V)
11*	183.31±1 (H)	13.2 × 15.5	1.25	B3	183.3±1 (V)
12	19.35 (H)	46.5 × 73.6	0.7	-	-
13	19.35 (V)	46.5 × 73.6	0.7	-	-
14*	22.235 (V)	46.5 × 73.6	0.7	A1	23.8 (V)
15	37 (H)	31.2 × 45.0	0.5	-	-
16*	37 (V)	31.2 × 45.0	0.5	A2	31.4 (V)
17*	91.655 (V)	13.2 × 15.5	0.9	B1	89 (V)
18	91.655 (H)	13.2 × 15.5	0.9	-	-

Polarization: V = Vertical; H = Horizontal; R = Right-hand Circular. Polarization for AMSU is at nadir. A1 and B1 stand for AMSU-A and B channel 1, respectively. Only F-16 uses V-pol on channels 1-5; F17 uses H.
* Channels used for the SSMIS precipitation retrievals.

In order for model-trained retrievals to perform well, there can be no TB biases between SSMIS and the model predictions used to train the retrieval algorithm. These biases were determined by aligning TB histograms for 26 globally distributed storms simultaneously viewed by F-16 SSMIS and modeled by MM5 as initialized using NCEP analyses. TBs were computed as for AMSU [1]. Each storm is ~950-km square. The two histograms were aligned at their highest TBs that matched at one order of magnitude below the average peaks of the two histograms (where the histograms are steep); examples are shown in Fig. 1. This matching only removes systematic biases, while validation of the model predictions is most sensitive when TBs are lowest, as shown in [1]-[2]. The resulting bias corrections were added to the observed SSMIS TBs. A global set of 122 storms [1] was used for training the precipitation estimator.

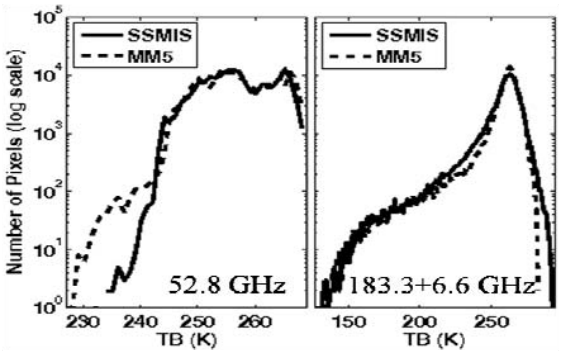

Fig. 1 Histograms of 52.8 and 183±6.6 GHz SSMIS and MM5 TBs aligned to yield the bias correction for SSMIS required to reconcile MM5 retrievals with SSMIS data.

Surfaces were classified as snow-free land, snow-covered land, ice-free sea, and sea ice, where snow and ice surfaces were classified using the AMSU surface classification algorithm [9] with some modifications providing best match between SSMIS and AMSU surface classes. Since surface emissivities of ice, snow, and frozen ground are complex and difficult to model, this first version of the SSMIS precipitation retrieval algorithm considers only snow-free land and ice-free sea with |lat| < 50º using separate algorithms called land and sea.

To reduce the sensitivity to surface emissivity and other unwanted geophysical variations, PCs were computed separately for land and sea surfaces using observed TBs for all orbits of day 13 of all months in year 2006 from SSMIS channels that correspond to AMSU-A channels 1-6 and 8, and AMSU-B channels 1-5. PCs offering good precipitation-to-noise ratios were identified and later used as inputs to the neural networks (NNs) that estimated precipitation. Good PCs for land are PC numbers 1 and 2, whereas those best for sea are PC numbers 2–5. Fig. 2 shows examples of PC1 for land and PC2 for sea.

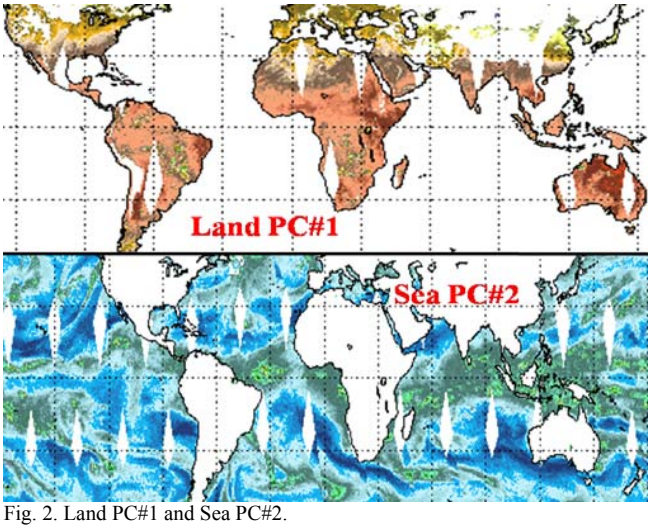

Fig. 2. Land PC#1 and Sea PC#2.

3. NEURAL NETWORK RETRIEVALS

The brightness temperatures (TBs) at 5-km resolution were simulated for 12 selected SSMIS channels described above using 122 MM5 global storms spanning a year; the same method was used in [1]. The FASTEM surface emissivity model [10] was used for sea and the assumed emissivity for land was uniformly distributed randomly between 0.91 and 0.97.

The neural network (NN) had 5, 3, and 1 neurons arranged in three layers; the last neuron was linear and those in the first two layers were sigmoidal. NNs were trained separately for land and sea surfaces, where the inputs included the good PCs described earlier. The best NN with the smallest rms errors of the ten NNs for each surface type was chosen. From the set of 122 MM5 storms, each of

which has 190×190 5-km pixels, 281,088 pixels were used for training (half for training and one quarter for each of testing and validation) and 269,498 other pixels were used for evaluation. The closest distance between any training and final evaluating pixel was ~14 km. NNs were trained to estimate MM5 surface precipitation rate (RR) at 15-km resolution.

4. RETRIEVAL RESULTS

Fig. 3 shows scatter plots between MM5 truth and SSMIS estimates separately for land and sea. Fig. 4 shows comparisons of the probability distributions over RR. Table II shows simulated rms, mean, and standard errors for land and sea for different RR ranges defined by MM5. Estimates for land are slightly less accurate than those for sea as evaluated using MM5 and all are useful for rates above ~1 mm/h. Fig. 5 shows comparisons of MM5-simulated and observed TBs for SSMIS ch. 9, MM5 RR, and RR estimated using MM5-simulated and SSMIS-observed TBs, respectively. The storms from left to right are over sea on 8/20/2006 at 10:06 UTC, and over land on 2/25/2006 at 11:55 UTC, respectively.

Fig. 6 compares annual precipitation estimates (mm/yr) for F-16 SSMIS, NOAA-15 AMSU [6], and Global Precipitation Climatology Project (GPCP) [11] for year 2006. NOAA-15 mean equatorial crossing times are ~2.5 hours ahead of F-16. GPCP data are 1-degree resolution and incorporate data from many satellites and rain gauges. SSMIS and AMSU annual totals were only from single satellites. SSMIS overestimates precipitation in under-vegetated land, e.g., in North Africa and the Middle East, because those estimates were not corrected for near-surface evaporation whereas AMSU data were. SSMIS estimates have less precipitation in several places, particularly for |lat| > 30º, partly because it has higher spatial resolution and resolves more precipitation, as illustrated in Fig. 7.

5. SUMMARY AND CONCLUSION

The first MM5-trained SSMIS precipitation retrieval algorithm was described, evaluated, and found to yield useful retrievals. MM5 comparisons suggest that SSMIS retrievals are useful above 1 mm/h for both land and sea. Comparison of F-16 SSMIS annual precipitation generally agrees with NOAA-15 AMSU and GPCP. Whereas SSMIS underestimates in several areas partly due to its higher spatial resolution, it overestimates over under-vegetated land due to near-surface evaporation.

6. ACKNOWLEDGMENT

The authors would like to thank Hilawe Semunegus and Axel Graumann at NOAA for providing us with SSMIS data.

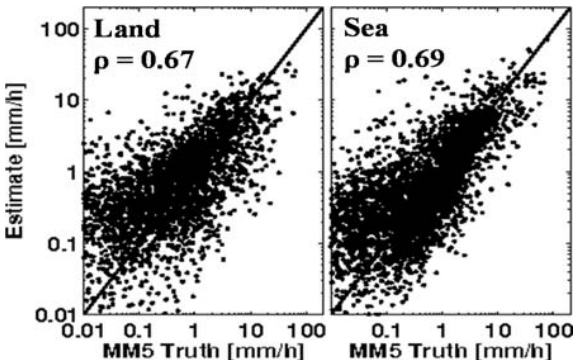

Fig. 3. Scatter plots between MM5 truth and SSMIS estimates for the evaluating pixels for land and sea.

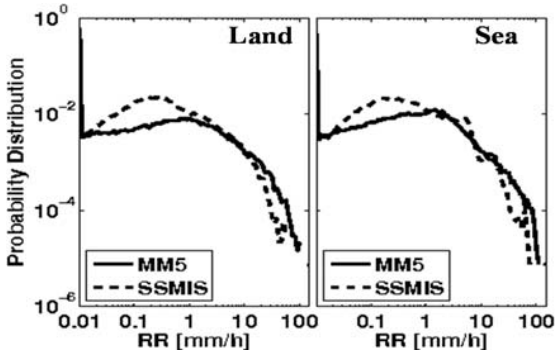

Fig. 4. MM5 and SSMIS RR probability distributions for the evaluating pixels of 122 MM5 storms for land and sea.

TABLE II
RMS, MEAN, AND STANDARD ERRORS (MM5 - ESTIMATE) FOR15-KM RESOLUTION MM5-SIMULATED SURFACE PRECIPITATION RATE RETRIEVALS (MM/H), WHERE THE RR RANGE IS DEFINED BY MM5

RR Range (mm/h)	RMS Error		Mean Error MM5-SSMIS		Standard Error	
	Land	Sea	Land	Sea	Land	Sea
0-0.125	*0.45*	*0.53*	*-0.19*	*-0.18*	*0.41*	*0.50*
0.125-0.25	*0.98*	*1.10*	*-0.41*	*-0.31*	*0.89*	*1.05*
0.25-0.5	*1.13*	*1.06*	-0.43	**-0.24**	*1.05*	*1.03*
0.5-1	*1.47*	*1.43*	**-0.44**	**-0.23**	*1.40*	*1.41*
1-2	1.94	1.63	**-0.36**	**-0.10**	1.90	1.63
2-4	2.62	2.47	**0.04**	**-0.28**	2.62	2.45
4-8	4.17	**3.75**	**1.28**	**0.29**	**3.97**	**3.74**
8-16	**7.72**	**6.99**	**4.98**	**3.52**	**5.90**	**6.04**
16-32	**15.27**	**14.39**	**13.12**	**10.66**	**7.83**	**9.67**
32-64	**28.91**	**28.46**	**26.37**	**24.18**	**11.88**	**15.03**
> 64	**58.31**	**56.42**	**53.04**	**52.10**	**24.72**	**21.81**

Italics highlights rms errors that exceed the upper bound listed in column 1 and therefore indicate poor utility. Boldface: rms errors below the range minimum listed in column 1.

7. REFERENCES

[1] C. Surussavadee and D. H. Staelin, "Comparison of AMSU Millimeter-Wave Satellite Observations, MM5/TBSCAT Predicted Radiances, and Electromagnetic Models for Hydrometeors," *IEEE Trans. Geosci. Remote Sens.*, vol. 44, no. 10, pp. 2667-2678, Oct. 2006.

[2] C. Surussavadee and D. H. Staelin, "Millimeter-Wave Precipitation Retrievals and Observed-versus-Simulated Radiance Distributions: Sensitivity to Assumptions," *J. Atmos. Sci.*, vol. 64, no. 11, pp. 3808-3826, Nov. 2007.

[3] C. Surussavadee and D. H. Staelin, "Global Millimeter-Wave Precipitation Retrievals Trained with a Cloud-Resolving Numerical Weather Prediction Model, Part I: Retrieval Design," *IEEE Trans. Geosci. Remote Sens.*, vol. 46, no. 1, pp. 99-108, Jan. 2008.
[4] C. Surussavadee and D. H. Staelin, "Global Millimeter-Wave Precipitation Retrievals Trained with a Cloud-Resolving Numerical Weather Prediction Model, Part II: Performance Evaluation," *IEEE Trans. Geosci. Remote Sens.*, vol. 46, no. 1, pp. 109-118, Jan. 2008.
[5] C. Surussavadee and D. H. Staelin, "Satellite Retrievals of Arctic and Equatorial Rain and Snowfall Rates using Millimeter Wavelengths," *IEEE Trans. Geosci. Remote Sens.*, vol. 47, no. 11, pp. 3697-3707, Nov. 2009.
[6] C. Surussavadee and D. H. Staelin, "Global Precipitation Retrievals Using the NOAA/AMSU Millimeter-Wave Channels: Comparison with Rain Gauges," *J. Appl. Meteorol. Climatol.*, vol. 49, no. 1, pp. 124-135, Jan. 2010.
[7] Northrop Grumman, "Algorithm and data user manual (ADUM) for the Special Sensor Microwave Imager/Sounder (SSMIS)," Technical Report, Jul. 2002.
[8] N. Sun, and F. Weng, "Evaluation of special sensor microwave imager/sounder (SSMIS) environmental data records," *IEEE Trans. Geosci. Remote Sens.*, vol. 46, no. 4, pp. 1006-16, Apr. 2008.
[9] N. C. Grody, F. Weng, and R. R. Ferraro, "Application of AMSU for obtaining hydrological parameters," in *Microwave Radiometry and Remote Sensing of the Earth's Surface and Atmosphere*, P. Pampaloni and S. Paloscia, Eds. Zeist, The Netherlands: VSP, 2000, pp. 339–352.
[10] S. J. English and T. J. Hewison, "Fast generic millimeter-wave emissivity model," *Proc. Int. Soc. Opt. Eng.*, vol. 3503, pp. 288–300, Aug. 1998.
[11] G. J. Huffman, R. F. Adler, M. M. Morrissey, D. T. Bolvin, S. Curtis, R. Joyce, B. McGavock, and J. Susskind, "Global precipitation at one degree daily resolution from multisatellite observations," *J. Hydrometeorol.*, vol. 2, no. 1, pp. 36–50, Feb. 2001.

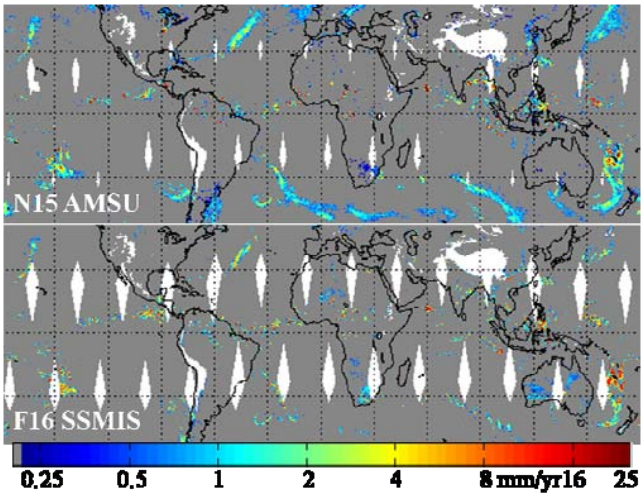

Fig. 7. Surface precipitation rate estimates (mm/yr) for NOAA-15-AMSU and F-16-SSMIS for 5/24/2006.

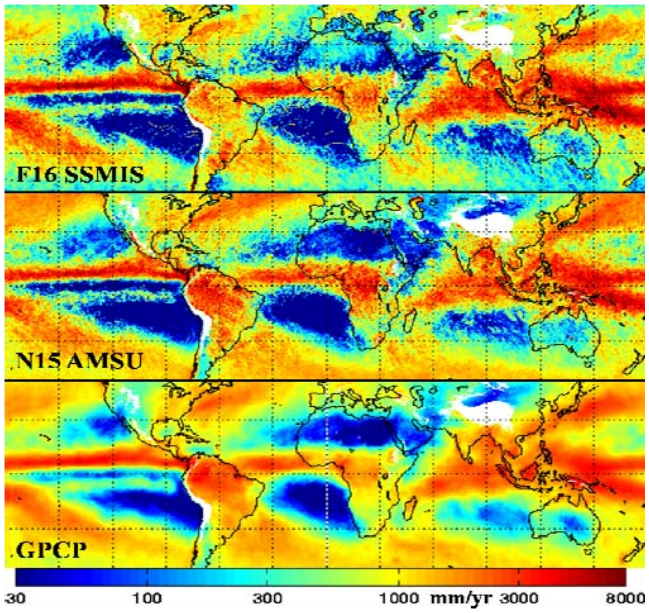

Fig. 6. Annual precipitation total (mm/yr) for F-16 SSMIS estimates, NOAA-15 AMSU estimates, and GPCP for year 2006.

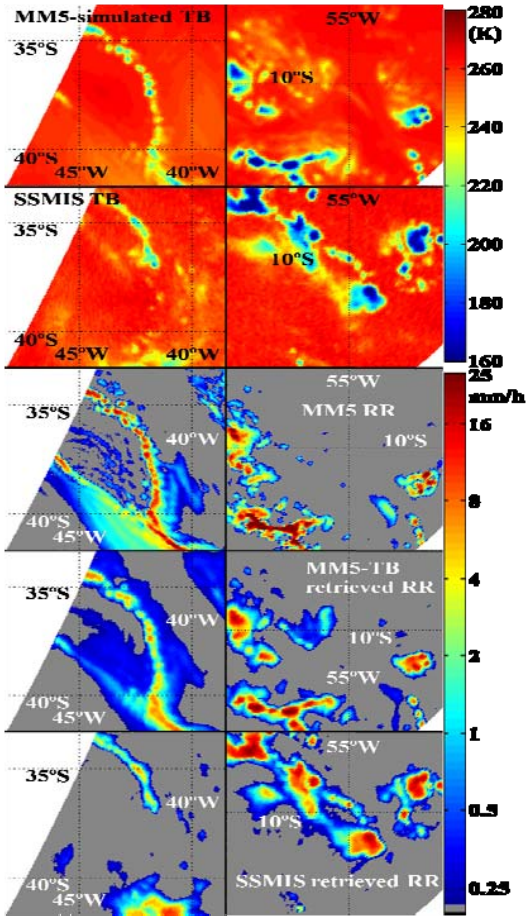

Fig. 5. Top to bottom: MM5-simulated and observed TB for SSMIS ch. 9, MM5 RR, and RR estimated using MM5-simulated and SSMIS-observed TBs. Left to right: storms over sea on 8/20/2006 at 10:06 UTC and over land on 2/25/2006 at 11:55 UTC, respectively.